Proceedings World Geothermal Congress 2000
Kyushu - Tohoku, Japan, May 28 - June 10, 2000

RECONSTRUCTION OF RESISTIVITY AND PERMITTIVITY PROFILES USING ELECTROMAGNETIC WELL LOGGING DATA

Jinsong Shen [1] , Yutaka Sasaki [1] , and Keisuke Ushijima [1]

[1] Geophysical Exploration Lab, Mining Engineering Dept., Faculty of Engineering, .Kyushu University, 6-10-1 Hakozaki, Higashi, Fukuoka, Japan, 812-8581

Keywords: EM tomography, resistivity and permittivity, electromagnetic well logging

ABSTRACT

There is low resistivity contrast between reservoir zone and host formation in geothermal fields, especially in areas where the technique of water injection is being carried out. Therefore, in low contrast area, permittivity can be one of the important reservoir indicators besides resistivity. In this study, one EM tomography method of reconstructing the resistivity and permittivity from electromagnetic well logging data was proposed. It was used to derive the distributions of resistivity and permittivity in nearby area around the borehole. The inversion procedures were carried out in two steps: first the low frequency EM well logging data was used to determine the resistivity, then it was regarded as the initial value, and the permittivity and resistivity were reconstructed from high frequency EM well logging data. The forward modeling at each inversion iteration was fulfilled by the numerical approximation of finite element method (FEM). Results of different anomalous bodies show that well logging data is only sensitive to nearby area around the borehole, the resolution of parameters is better in vertical direction than that in horizontal direction though it is also related to the distance between transmitter and receiver. Numerical simulation also suggests that as the frequency increases, the sensitive range becomes small. From our results, it can be said that the method proposed in our study can simultaneously reconstruct permittivity and resistivity from multi-frequency EM well logging data, and it may be a valuable means of evaluating low resistivity contrast reservoir in geothermal fields as well as in oil fields.

1. INTRODUCTION

Although imaging results of cross-well electromagnetic data have been widely investigated and applied in study of subsurface geological structure, rock porosity, fluid saturation and fracture evaluation, the inversion of well logging data, with higher vertical resolution, has not been studied so much up to now. Furthermore, little has been done on the problem of simultaneous reconstruction of resistivity and permittivity profile in a well logging environment. In practice, EM well logging is carried out almost in every borehole, therefore it is important to develop an effective method of EM well logging inversion. On the other hand, there are areas with low resistivity contrast between reservoir zone and host formation in geothermal fields, especially in areas where the technique of water injection is carried out. The permittivity of water is much bigger than that of host rock commonly present in subsurface formations. Therefore, in low contrast areas, permittivity can be one of the important reservoir indicators besides resistivity.

In this study, an EM tomography method for deducing the resistivity and permittivity from EM well logging data was developed. It was used to obtain the distribution of resistivity and permittivity in nearby area around the borehole. In the inversion process, the regularized least-squares inversion scheme is used to solve the ill-posed problem. The inversion procedure was carried out in two stages. First the induction logging data was used to determine the resistivity distribution, then it was used as an initial model, and the permittivity and resistivity were inverted simultaneously from high frequency EM well logging data. In simulation, a vertically oriented magnetic dipole is used as a source, and the medium in the calculated area is assumed to be azimuthally symmetric about the dipole source axis. The forward modeling at each inversion iteration was accomplished by FEM.

Several kinds of profiles were simulated and inverted with the method. Inversion results for different anomalous bodies show that well logging data is only sensitive to nearby area around the borehole, the resolution of parameters is better in vertical direction than that in horizontal direction, though it is also related to the distance between transmitter and receiver. Numerical simulation also suggests that as the frequency increases, the sensitive range becomes small.

2. RESPONSE OF EM WELL LOGGING

With respect to EM well logging, here we limit our discussion to induction log and the electromagnetic propagation well logging. Figure 1 shows the schematic concept of our single borehole tomography system.

For induction log, we only write out the response of the probe with one transmitter and one receiver. In order to calculate the apparent conductivity, the electromotive force induced in receiver must be derived from electromagnetic field. The electromotive force in the receiver can be calculated through two ways, one is from electric field $E_{\ddot{O}}$, another is from the vertical magnetic field in Z direction. If we denote electromotive force as Ψ, following formulae can be derived when the radius of the transmitter and receiver coils is very small:

$$\Psi = \oint_l E_\Phi dl N_R = 2\pi r_R E_\Phi N_R \qquad (1)$$

or $$\Psi = i\omega\mu \iint H_z dS N_R = i\omega\mu\pi r_R^2 H_z N_R \qquad (2)$$

where r_R is the radius of the receiver coil, N_R is the turns of the receiver coil.

By using electromotive force Ψ, apparent conductivity can be derived using the following equations

$$\sigma_a^R = -\frac{\mathrm{Re}(\Psi)}{K} \text{ and } \sigma_a^X = -\frac{\mathrm{Im}(\Psi_m - \Psi)}{K} \qquad (3)$$

where Ψ_m is the coupling electromotive force between transmitter and receiver in free space

$$\Psi_m = -i\omega\mu \frac{M_T M_R}{2\pi L^3} \qquad (4)$$

where $M_T = N_T \pi r_T^2 I$ and $M_R = N_R \pi r_R^2$ are moments of transmitter and receiver respectively; K is the instrument factor

$$K = \frac{(wm)^2 (p r_T^2)(p r_R^2) N_T N_R}{4pL} I \quad (5)$$

where, radian frequency $w = 2pf$, s_a^R is the apparent conductivity of the resistive signal, s_a^X is the apparent conductivity of reactive signal, r_T and r_R are radius of the transmitter and receiver coils respectively, N_T and N_R are the turns of the transmitter and receiver coils respectively, L is the spacing between the transmitter and receiver, f is the frequency of the transmitter current, I is the intensity of the transmitter current, m is the magnetic permeability of the medium.

Regarding to the dielectric logging tool, we consider the three probe coils, one transmitter and two receivers. And the responses are amplitude attenuation and phase difference between the two receivers. If the electromotive forces in two receivers are Ψ_1 and Ψ_2, then amplitude attenuation and phase difference can be written

$$A = 20\log(\frac{\Psi_1}{\Psi_2}) \text{ (dB) and } \Delta\Phi = \mathrm{Im}\left[\ln(\frac{\Psi_1}{\Psi_2})\right] \quad (6)$$

where A is amplitude attenuation and $\Delta\Phi$ is phase difference.

From above discussion, we can see that, the output signal of both the induction well log and the EPT well log are related to electromotive force in receiver, that is related to magnetic field component in vertical direction. So we only need to deal with how to obtain H_z.

3. CALCULATION OF ELECTRIC AND MAGNETIC FIELDS BY FEM

In this study we assumed the well logging environment to be a symmetric cylindrical geometry shown in Figure 2. Under the assumption of axis-symmetry, the electric field of the dipole transmitter has only one tangential component E_f and is governed by the following equation

$$\frac{\partial^2 E_f}{\partial z^2} + \frac{\partial}{\partial r}\left[\frac{1}{r}\frac{\partial}{\partial r}(rE_f)\right] + k^2 E_f = iwmJ_f \quad (7)$$

where, $k^2 = w^2 m(e_0 e_r - i\frac{s}{w})$

The magnetic field of the vertical component H_z and can be calculated from E_f

$$H_z = -\frac{1}{iwm}\left[\frac{1}{r}\frac{\partial}{\partial r}(rE_f)\right] \quad (8)$$

where $w = 2pf$ radian frequency, f the frequency, e_0 the permittivity of the free space, e_r the relative permittivity of the medium, s the conductivity of the medium and m the magnetic permeability of the medium.

For computational efficiency and accuracy, we separate the total field into two parts, that is primary field E_p and scattering field E_s, and is given by

$$E_f = E_p + E_s \quad (9)$$

Correspondingly, the total vertical magnetic field H_z can also be separated into two parts, primary magnetic field H_z^p and secondary magnetic field H_z^s as follows:

$$H_z^p = -\frac{1}{iwm}\left[\frac{1}{r}\frac{\partial}{\partial r}(rE_P)\right]$$

and $H_z^s = -\frac{1}{iwm}\left[\frac{1}{r}\frac{\partial}{\partial r}(rE_s)\right]$ (10)

In this study, we assume that the primary field is excited by the magnetic dipole in a homogeneous whole space having the parameters of the environment where the transmitter resides (either that of the borehole mud or a bed medium when there is no borehole). So we only need to consider the computation of the scattering field by FEM. The scattering field is the difference between the total field and the primary field. From equation (9) we have

$$\frac{\partial^2 E_s}{\partial z^2} + \frac{\partial}{\partial r}\left[\frac{1}{r}\frac{\partial}{\partial r}(rE_s)\right] + k^2 E_s + (k^2 - k_0^2)E_P = 0 \quad (11)$$

The variational integral of the differential equation (11) is

$$J(E_s) = \iint_s \left\{\left[\frac{1}{r}\frac{\partial}{\partial r}(rE_s)\right]^2 + \left[\frac{\partial E_s}{\partial z}\right]^2 - k^2 E_s^2 - 2(k^2 - k_0^2)E_s E_p\right\} r dr dz \quad (12)$$

Based on the variational principle, the solution E_s to the differential equation is the function that makes the variational integral $J(E_s)$ stationary.

4. THE REGULARIZED LEAST-SQUARES INVERSION SCHEME

Because the observed well logging data set is always not equal to the number of the unknown parameters, the inversion process is non-unique, unstable and ill-posed, and the available estimation is only possible in least-squares sense with regularization (Tikhonov and Arsenin,1977). Regularization excludes solutions that are too rough by imposing a roughness constraint on the data fit. Reconstruction is smoothed at the expense of an increase in the fitting error. Let the data be denoted generically by the vector D, and the model by the parameter vector m, to carry out forward modeling to generate theoretical responses and also to solve the inverse problem. We divide our model into N rectangular cells and assume that the conductivity is constant within each cell. Our inverse problem is solved by finding the vector $m = \{m_1, m_2 \cdots\cdots m_N\}$, which adequately reproduces the observed data $D^o = \{D_1^o, D_2^o \cdots\cdots D_M^o\}$ with an acceptable RMS (root of mean squares) misfit. If it is expressed in mathematical form, our inverse procedure is to minimize the following function and to get a smooth reconstruction of model parameters

$$\Phi = \left\|W_D(D^c - D^o)\right\|^2 + m\left\|W_m m\right\|^2 \quad (13)$$

where D^o is observed data set, D^c is calculated data set, m is model parameter set, W_D and W_m are data weighting and parameter weighting matrix respectively, and m is the Lagrangian multiplier which controls the degree of the smoothness, corresponding to the minimum error through the interpolation of all the residual errors. In order to enhance the stability of the inversion and get a meaningful result, we further used the bound constraints by solving equation (13) subject to the condition:

$$L \le m \le U \qquad (14)$$

where L and U are lower and upper bounds of the parameter vector m respectively.

Because the information of horizontal resolution is contained in the large offset measurements, at a specific frequency, the data of the large offset are several orders of magnitude smaller than that of the small offset data. If we directly use the raw data in inversion, the imaging process has difficulty to recover the lateral position of the anomalous bodies. In this study, we solve this problem by weighting each source-receiver combination equally, and normalize the complex field data by its amplitude. Performing this operation prior to inversion process numerically removes the attenuating effects of the background medium and provides better horizontal resolution of the scattering bodies.

5. SENSITIVITY OF VERTICAL MAGNETIC FIELD TO RESISTIVITY AND PERMITTIVITY

From the response equations of induction and EPT well logging, we can see that all the responses are directly related to vertical component of magnetic field. For the ease of discussion, in the following context we only deal with sensitivities of the vertical magnetic field to resistivity and permittivity. In this study, we use the same equation adopted in the method of Ward and Hohmann (1988). For the perturbed medium, the total vertical magnetic field H_{z2} measured in the receiver borehole some distance from the source can be expressed as

$$H_{z2} = H_{z1} + \iint_D (k_2^2 - k_1^2) E_{f2} G_{Hz1} dr dz \qquad (15)$$

where $k_1^2 = w^2 m(e_{r1} e_0 - i\frac{1}{r_1 w})$, H_{z1} and H_{z2} are vertical magnetic fields before and after the medium is perturbed, E_{f2} total electric field after the medium is perturbed and G_{Hz1} is adjoint Green's function, k_2^2 and k_1^2 are complex wavenumbers of the medium before and after it is perturbed, D is the area of the perturbation block.

The response change caused by the perturbation can be expressed as:

$$\Delta H = \iint_D \Delta k^2 (E_{f1} + \Delta E_f) \times G_{Hz1} dr dz \qquad (16)$$

where E_{f1} is the total electric field before the medium is perturbed. When the block and perturbation are small, Δk^2 can be regarded as constant in domain D, and also $E_{f1} > \Delta E_f$, so we can use the first order Born approximation and obtain

$$\Delta H = \Delta k^2 \iint_D E_{f1} G_{Hz1} dr dz \qquad (17)$$

From equation(17), we can get the sensitivity of response H_z to resistivity and permittivity at wave number k_1^2:

$$\frac{\partial H_z}{\partial r} = \frac{iwm}{r^2} \iint_D E_{f1} G_{Hz1} dr dz \qquad (18)$$

$$\frac{\partial H_z}{\partial e_r} = w^2 m e_0 \iint_D E_{f1} G_{Hz1} dr dz \qquad (19)$$

In equation (18) and (19), the electric field E_{f1} can be calculated by FEM, while the whole space Green's function G_{Hz1} has to be calculated for every block D, and is computational intensive. In fact, G_{Hz1} is the magnetic field at receiver point when the dipole sources are put at the nodes within D block, based on the principle of reciprocity, it is equal to the weighted sum of the fields at the nodes within D block when the dipole source is at receiver location. Usually the number of receiver stations is less than that of inversion blocks, so sensitivities can be calculated efficiently by using the principle of reciprocity.

In this study, we calculated G_{Hz1} through the total electric field caused by point source at receiver by following equation:

$$G_{Hz1} = -\frac{1}{iwm}\left[\frac{1}{r}\frac{\partial}{\partial r}\left(rE_f^R\right)\right] \qquad (20)$$

where, E_f^R is the total electric field in block location when the dipole source is located at receiver point.

6. NUMERICAL RESULTS

Numerical results of several kinds of models were obtained to verify the effectiveness of our forward code and inversion method. First we compare our forward results with the published results that were derived from analytical or numerical methods of typical models, then several models were reconstructed by our inversion method.

6.1. Validation of The Forward Code

Figures 3(a) and (b) show the comparison of FEM apparent conductivity of the two-coil induction probe in four-layer model with no borehole effect, and the analytic solution. We can see that FEM results agree well with that of the analytic solution.

Figures 4(a) and (b) show amplitude attenuation and phase difference of the three-coil dielectric well logging probe calculated by FEM and that obtained by Chew et al(1984) using numerical mode matching method (NMM). The operating frequency is $25MHz$ and the spaces of $T - R_1$ and $T - R_2$ are 25 and 50 inches respectively.

6.2. Reconstruction Results

Figure 5 shows the model to be simulated and the reconstructed profile. The model consists of two 2.0×2.0 m square bodies located 0.5 m from the borehole and 2 m separated in vertical direction, the resistivity of the bodies is 10Ωm and the resistivity of the host rock is, 10 times that of the body, 100Ωm. With 40 transmitter positions, 80 measurements spaced at 0.5 m in the interval of 20 m depth. Therefore the data set to be inverted is 80 measurements. The whole calculation area was divided into 100×100 cells, and the inversion area is limited to the central part of the whole calculation area (represented with black border in Figure 5a) and divided into 23×19 blocks, the block size is $0.5\,m \times 0.5\,m$, the operating frequency is $20kHz$, the imaging result was in the right part of this figure. We can see that the anomalous body was well resolved.

In order to test the resolution in horizontal direction, two-

block model similar to that in Figure 5, except that the distance from borehole is 1.5 m, was simulated. Figure 6 shows the model and the inversion result. We can see that though the two bodies were distinguished well, the right boundary and the intermediate part of the anomalous body were not as good as that in Figure 5.

Figure 7 presents similar model to that in Figure 6, with the anomalous bodies spaced 4.0 m in vertical direction and 2.0 m from the borehole in horizontal direction. Their reconstruction is shown in the right part. We can see that though the two anomalous bodies were reconstructed in the correct position, their sizes and boundaries were not so clear as that in Figure 6.

Figure 8 indicates a similar model to that in Figure 5, with the anomalous bodies aligned in horizontal direction, with 2.0 m separation. Their reconstruction is presented in the right part. From this result, we can only obtain one big anomalous body with blur boundary.

Figure 9 presents similar model to that in Figure 5, with the host rock $10\Omega m$, anomalous bodies are $100\Omega m$, in order to test the adaptability to low host resistivity. The good reconstruction is shown in the right part. We can see that while the anomalous body was well resolved, its size is smaller than that of the model, because of the background attenuation.

Figure 10 indicates a model of one vertical fracture in homogeneous medium and its inversion result. We can see that the low resistivity fracture was well resolved.

Figure 11 shows the model similar to that in Figure 5, with the resistivity and relative permittivity of the bodies are $10\Omega m$ and 35 respectively, the resistivity and relative permittivity of the host rock are $100\Omega m$ and 5. The inversion result in Figure 5b used as an initial model to simultaneously resolve resistivity and permittivity, the working frequency is $20MHz$. The inversion block size is $0.5m \times 0.5m$, the reconstruction of permittivity profile was shown in the right part of this figure. We can see that though the permittivty anomaly was resolved, its size and boundary were not so accurate as that of the resistivity result.

Figure 12 indicates similar model to that of Figure 9, with the relative permittivity of the anomalous bodies 5, that of the host rock is 50. The reconstructed permittivity profile discerned the anomaly but was not very clear.

From Figures 11b and 12b, we can see that, though not as good as resistivity image, the reconstructed permittivity profile gives the correct location and reasonable boundary of the anomalous body .

7. CONCLUSION

In this study, it is shown that the regularized least-squares inversion method using the FEM can effectively reconstruct resistivity and permittivity profiles from electromagnetic well logging data in the nearby area around the borehole. Numerical simulations indicate that induction logging data can provide good resistivity distribution profiles, while the high frequency electromagnetic well logging measurements can give permittivity and resistivity profiles simultaneously. From our inversion results, it can be said that EM well logging data inversion may be valuable means of evaluating low resistivity contrast and fracture reservoirs. Test results also suggest that the area distant from the source and receiver well presents low resolution of resistivity and permittivity images. While in the nearby area around the borehole, parameter images can be obtained with high resolution. Our future study will be on the use of multi-frequency and multi-component measurements to enhance the inversion stability, and on the use of non-reflection absorbing boundary condition to reduce the mesh size and increase the computational efficiency.

ACKNOWLEDGMENTS

The authors wish to thank two reviewers for their constructive criticism that improved this paper to its present form.

REFERENCES

Alumbaugh, D. L., and Morrison, H. F., 1995, Theoretical and practical considerations for cross-well electromagnetic tomography assuming a cylindrical geometry: Geophysics, **60**, 846-870.

McGillivray, P. R., Oldenburg, D. W., Ellis, R. G., and Habashy, T. M., 1994, Calculation of sensitivity for the frequency-domain eletromagnetics: Geophys. J. Int., **116**, 1-4.

Chang, Shu-Kong, and Anderson, B., 1984, Simulation of induction log by the finite-element method: Geophysics, **49,** 1953-1958.

Tikhonov, A.N., and Arsenin, V.Y., 1977, Solutions of ill-posed problems: John Wiley and Sons, Inc.

Ward, S. H., and Hohmann, G. W., 1988, Electromagnetic theory for geophysical applications, in Nabighian, M. N., Ed., Electromagnetic methods in applied geophysics theory, Vol.1: Soc. Explor. Geophys., 131-311.

Chew, W. C., Barone, S., Anderson, B., and Hennessy, C., 1984, Diffraction of axi-symmetric waves in a borehole by bed boundary discontinuities: Geophysics, **49**, 1586-1595.

Sasaki, Y., Matsuo, K., and Yokoi, K., 1994, Resistivity inversion of cross-hole and borehole-to-surface EM data using axially symmetric models: Geophysical Prospecting, **42**, 745-754.

Zhou, Q., Becker, A., and Morrison, H. F., 1993, Audio-frequency electromagnetic tomography in 2-D: Geophysics, **58,** 482-495.

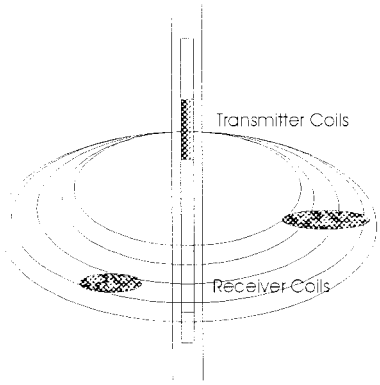

Figure 1 The schematic concept of the single borehole tomography system

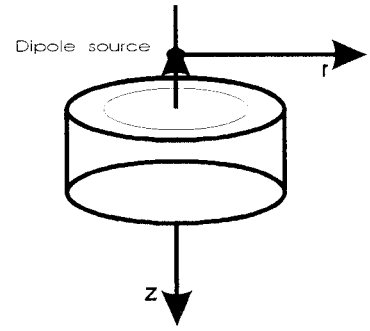

Figure 2 Symmetric cylindrical geometry for EM well logging problem

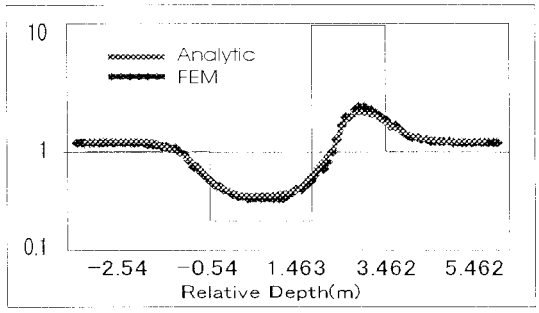

(a)Resistive Signal of Induction Log(20kHz)

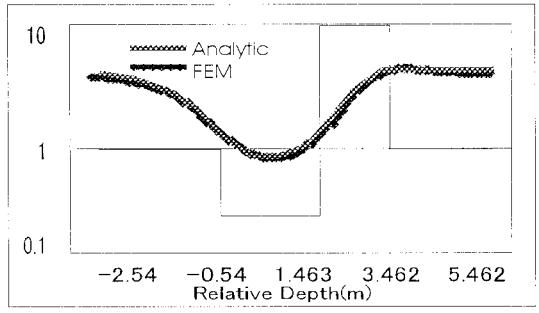

(b)Reactive Signal of Induction Log(20kHz)

Figure 3 Comparison of FEM results with analytic responses of Induction Log in four layer formation

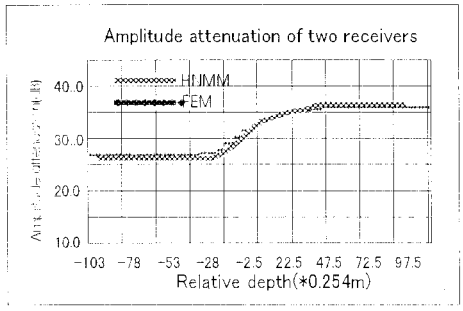

(a) Ratio of amplitude attenuation of two receivers

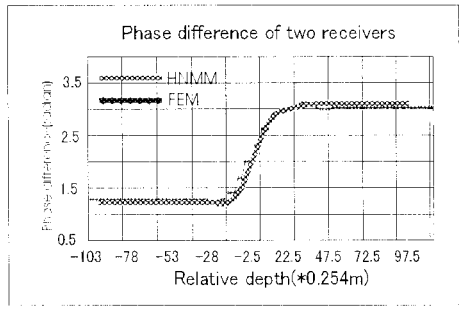

(b) Phase difference of two receivers

Figure 4: Comparison of FEM results with that of HNMM(horizontal numerical mode matching) method

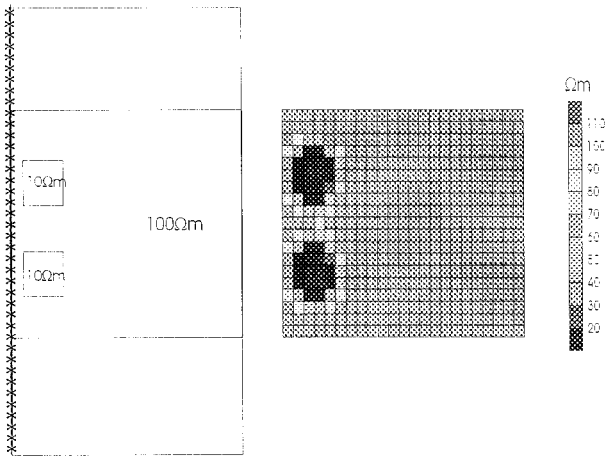

Figure 5 Model and inversion result of two vertical blocks (separation is 2.0 m between anomalous bodies, 0.5 m from borehole)

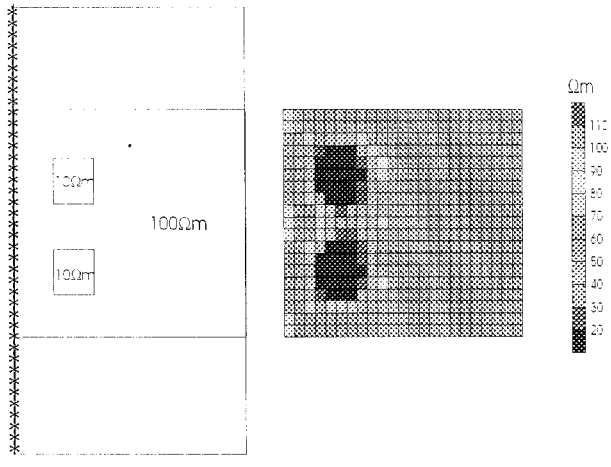

Figure 6 Model and inversion result of two vertical blocks (separation is 2.0 m between anomalous bodies, 1.5 m from the borehole)

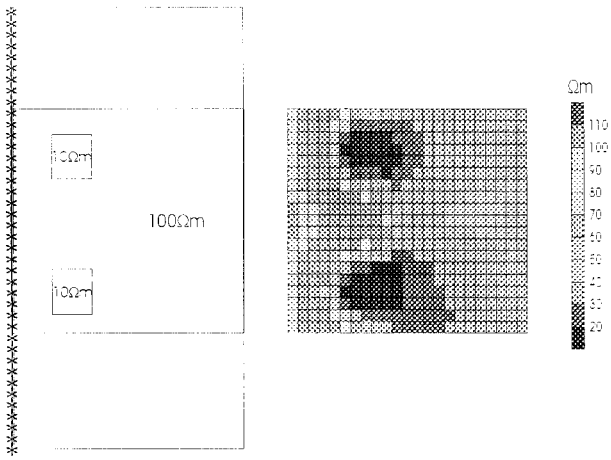

Figure 7: Model and inversion result of two vertical blocks (separation of anomalous bodies is 4.0 m, both are 2.0 m from the borehole)

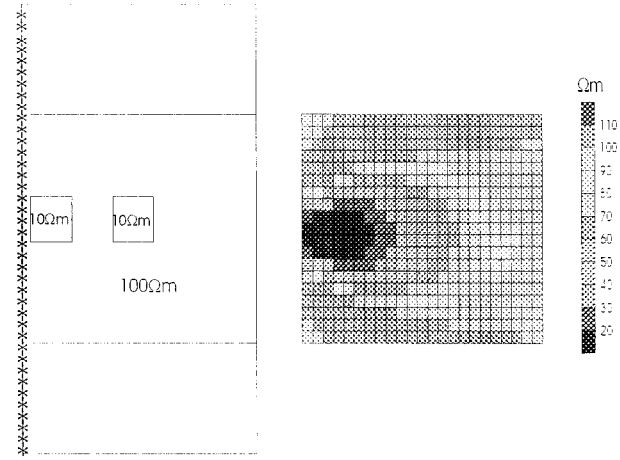

Figure 8 Model and inversion result of two horizontal blocks(separation of anomalous bodies is 2.0 m, the first block is 0.5 m from the borehole)

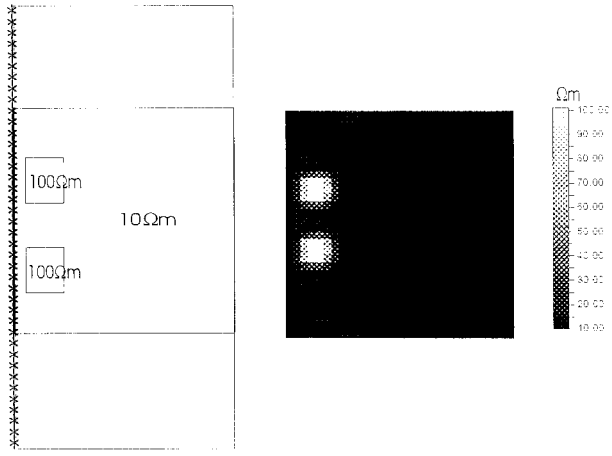

Figure 9 Model of low resistivity host rock and inversion result of two vertical blocks(separation of anomalous bodies is 2.0 m, both are 0.5 m from the borehole)

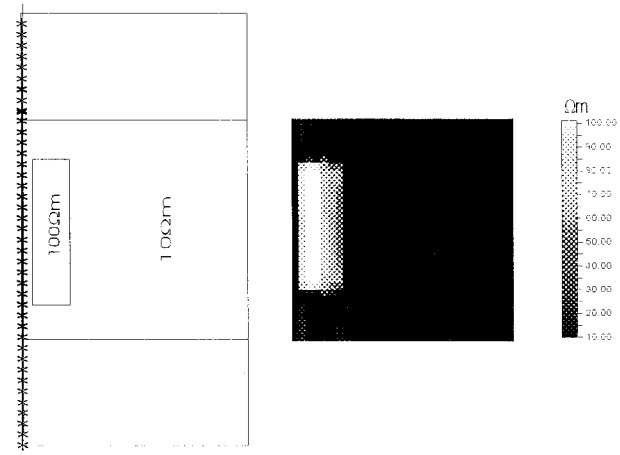

Figure 10 Model of one vertical fracture nearby the borehole and the inversion result

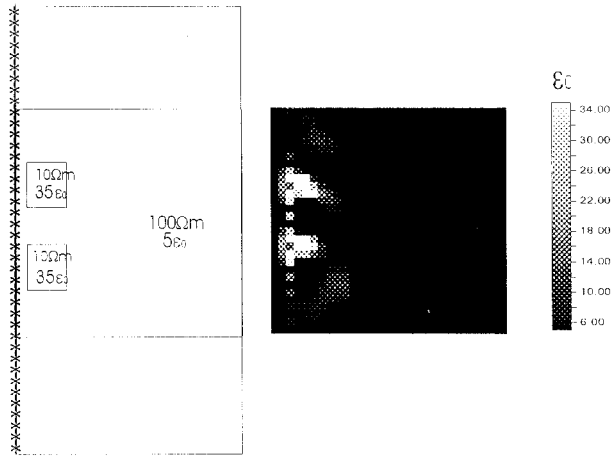

Figure 11 Model and inversion result o f high frequency (20MHz) EM data of two vertical blocks (separation of anomalous bodies is 2.0 m, both are 0.5 m from the borehole)

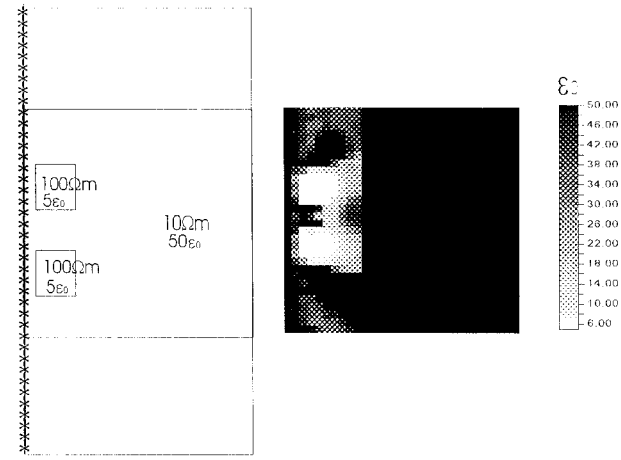

Figure 12 Model and inversion result o f high frequency (20MHz) EM data of two vertical blocks (separation of anomalous bodies is 2.0 m, both are 0.5 m from the borehole)